Journal of Hazardous Materials Advances 4 (2021) 100018

Contents lists available at ScienceDirect

Journal of Hazardous Materials Advances

journal homepage: www.elsevier.com/locate/hazadv

Cometabolic benzo[*a*]pyrene biotransformation by *Sphingobium barthaii* KK22 proceeds through the kata-annelated ring and 1-pyrenecarboxylic acid to downstream products.

Minami Izawa, Miharu Sakai, Jiro F. Mori, Robert A. Kanaly*

Department of Life and Environmental System Science, Graduate School of Nanobiosciences, Yokohama City University, 22-2 Seto, Kanazawa, Kanagawa, Yokohama 236-0027

ARTICLE INFO

Keywords:
Cometabolism
Benzo[a]pyrene
Sphingobium
Polycyclic aromatic hydrocarbons
Biotransformation

ABSTRACT

Benzo[*a*]pyrene is a hazardous environmental pollutant that is resistant to bacterial biodegradation and biotransformation pathway development has not been advanced. Considering this, cometabolic benzo[*a*]pyrene biotransformation by a member of the genus *Sphingobium* was investigated by cell growth on phenanthrene as a carbon and energy source in conjunction with comparative analyses of culture extracts by gas chromatography (GC) and liquid chromatography electrospray ionization tandem mass spectrometry (LC/ESI-MS/MS). Under these culture conditions, approximately 20% of 100 mg/L benzo[*a*]pyrene (apparent solubility) was biodegraded in 14 days and benzo[*a*]pyrene biotransformation products were detected and identified to be extradiol and intradiol ring-cleavage products of the benzo[*a*]pyrene kata-annelated ring. The *o*-hydroxy-tetraaromatic acids, 2-hydroxypyrene-1-carboxylic acid, and 1-hydroxypyrene-2-carboxylic acid were identified in addition to 7,8- and 9,10-dihydroxy-benzo[*a*]pyrenes, carboxyvinylpyrene-carboxylic acids, hydroxypyrene-oxobutenoic acids, pyrene-1,2-dicarboxylic acid, 1,2-dihydroxypyrene and different oxophenalene compounds. 1-Pyrenecarboxylic acid and other ring-opened oxidized compounds were identified as novel benzo[*a*]pyrene biodegradation products. In separate assays, 2-hydroxypyrene-1-carboxylic acid was found to be produced from 1-pyrenecarboxylic acid and these results reshaped our understanding of bacterial benzo[*a*]pyrene biotransformation pathways. Overall, the identities of thirteen products were proposed and new benzo[*a*]pyrene biodegradation pathways were constructed from experimental chemical evidence. This work extends our understanding of benzo[*a*]pyrene biotransformation by gram-negative bacteria.

Introduction

Detection and identification of biotransformation products from the bacterial biodegradation of hazardous high molecular weight polycyclic aromatic hydrocarbons (HMW PAHs) provides valuable information for understanding the mechanisms by which these compounds may be transformed (Juhasz and Naidu, 2000; Kanaly and Harayama, 2000). This knowledge is applicable to predicting PAH transport and fate in the environment, to risk assessment and mitigation methods and to the development of strategies for biological upgrading of heavy oils (Leon and Kumar, 2005; Lundstedt et al., 2007; Haritash and Kaushik, 2009; Fernandez-Luqueno et al., 2011; Podgorski et al., 2021; Tomiyama et al., 2021). Additionally it provides data support to large-scale metabolomics investigations as has been shown recently (Tian et al., 2018).

At the same time, when cometabolism is involved in hazardous pollutant biotransformation, detection and identification of products poses challenges because products originating from the cometabolically-metabolized substrate, i.e., the secondary substrate, must be differentiated from the products of the primary substrate(s). In the case of HMW PAH cometabolism, the structural similarities of primary and secondary substrates combined with the structural similarities among downstream biotransformation products from both substrates further complicates matters when attempting to separate and assign identities to unknown biotransformation products derived from the secondary substrate (van Herwijnen et al., 2003; Zhong et al., 2007, 2011; Toyama et al., 2011; Zeng et al., 2019).

Benzo[*a*]pyrene is a five-ring HMW PAH that is a constituent of heavy oil and oily sludges, may damage cellular nucleic acids and proteins and is regarded as a relatively persistent compound that when biodegraded by bacteria is generally only biodegraded under cometabolic conditions (Goto et al., 1997; Juhasz and Naidu, 2000; Frank et al., 2002; Kriipsalu et al., 2008; Verma et al., 2012; Penning, 2014; Takeshita and Kanaly, 2019). Due to the apparent limited types of bacteria that may significantly biodegrade benzo[*a*]pyrene

* Corresponding author.
E-mail address: kanaly@yokohama-cu.ac.jp (R.A. Kanaly).

https://doi.org/10.1016/j.hazadv.2021.100018
Received 3 July 2021; Received in revised form 31 August 2021; Accepted 14 October 2021

combined with the cometabolic nature of its metabolism, there are few reports of benzo[*a*]pyrene biotransformation mechanisms where experimental chemical evidence has been provided for the construction of biodegradation pathways (Fu et al., 2014). In the last 25 years there have been various studies which document benzo[*a*]pyrene biodegradation under different conditions including in soil, by bacterial consortia and sometimes by defined isolates or groups of isolates (Juhasz and Naidu, 2000; Kanaly and Harayama, 2000, 2010; Song et al., 2015; M'Rassi et al., 2015; Folwell et al., 2016; Yan et al., 2017; Zhu et al., 2017). Even so, there have only been two reports where multiple (at least three or more) biotransformation products were identified from a single organism under aerobic conditions by experimental chemical evidence and this situation has limited our understanding of benzo[*a*]pyrene biotransformation mechanisms and hindered biodegradation pathway development (Schneider et al., 1996; Moody et al., 2004). In the above-mentioned reports, the organisms involved in benzo[*a*]pyrene biodegradation were both Gram-positive members of the genus *Mycobacterium* and it was shown that molecule oxidation and ring-opening occurred through the 4,5-, 7,8- and 9,10-carbon positions to produce tetraaromatic metabolites (Schneider et al., 1996; Moody et al., 2004); reports of biotransformation products from non-actinomycete organisms are few (Gibson et al., 1975; Rentz et al., 2008).

In this investigation, *Sphingobium barthaii* KK22 cells were exposed to phenanthrene or phenanthrene plus benzo[*a*]pyrene with the purpose to identify benzo[*a*]pyrene biotransformation products to construct more comprehensive biodegradation pathways for prokaryotes.

Materials and methods

Chemicals, bacterial strain and growth media

Phenanthrene (98% purity) and 1-pyrenecarboxylic acid (97% purity) were purchased from Sigma-Aldrich (St. Louis, MO, USA). Benzo[*a*]pyrene (>97% purity), pyrene (>98% purity), *N,N*-dimethylformamide (DMF; >99% purity), chloroform, ethyl acetate and methanol (HPLC grade or higher) were purchased from Wako Pure Chemical Industries (Osaka, Japan).

Sphingobium barthaii strain KK22 (Maeda et al., 2015) was isolated from a soil consortium and details of the consortium, strain KK22 and their maintenance are described elsewhere (Kanaly et al., 1997; 2000; 2001; Kanaly and Watanabe, 2004; Kunihiro et al., 2013).

*Quantitative analyses of phenanthrene and benzo[*a*]pyrene biodegradation by strain KK22*

S. barthaii KK22 cells were grown on 20 mM glucose in 1-L volume conical flasks that contained 200 ml of Stanier's Basal Medium (SBM; Atlas, 1993) by continuous rotary shaking at 150 rpm at 30 °C in the dark. After 24 h, cells were washed in phosphate buffer (PBS; 50 mM, pH 7.1), twice pelleted by centrifugation (8700 x *g*, 10 min, 4 °C), resuspended in SBM and transferred into 18-ml volume glass tubes that contained five ml of SBM and benzo[*a*]pyrene and/or phenanthrene at concentrations of 100 mg/L each (apparent solubility). PAHs were transferred in DMF before the addition of cells (final cell densities = 0.4). Cell growth was measured by spectrophotometer (V-530 model, Jasco, Tokyo, Japan) whereby culture fluids in 600 µl aliquots were aseptically removed and measured in a quartz cuvette. At the start of incubation and after 14 days, cultures were sacrificed in triplicate by whole tube extraction with equal volumes of chloroform plus addition of pyrene in chloroform as an extraction standard. Tubes were shaken for 18 h in the dark at 23 °C by reciprocal shaking and extracted two times further with chloroform. Extracts were pooled, passed through anhydrous sodium sulfate into 250-ml volume glass evaporating flasks and concentrated in vacuo by rotary evaporation (Eyela model N-1000, Tokyo Rikakikai Co., Ltd., Tokyo, Japan). Finally, extracted material was resuspended in 1 ml of chloroform and transferred to 2-ml volume amber glass vials.

Extracts were analyzed by gas chromatography (GC; GC-2014, Shimadzu, Kyoto, Japan) equipped with a capillary column (ZB-5, Phenomenex, CA, USA; 30 m x I.D. 0.25 mm x 0.25 µm). The carrier gas was helium and the flow rate was 1.0 ml per min. The injector temperature was 280 °C and the detector temperature was 300 °C. The temperature program was as follows: 150 °C for 2 min followed by continuous increase of 10 °C per min to 280 °C, and a final holding temperature of 280 °C for 10 min for 25 min total run time. Sample injection volumes were typically 1 µl and were applied manually by a 10-µl glass microsyringe fitted with a Chaney adaptor (Hamilton, Reno, NV, USA). Peak areas and retention times were determined by GC solution software version 2.4 (Shimadzu, Kyoto, Japan). Under these conditions, phenanthrene eluted at 9.5 min, pyrene eluted at 12.9 min and benzo[*a*]pyrene eluted at 21.1 min. The recoveries of each PAH were calculated based upon calibration curves for authentic standards of phenanthrene, benzo[*a*]pyrene, and pyrene that were constructed under identical GC conditions.

*Monitoring benzo[*a*]pyrene biotransformation in large volume cultures*

Strain KK22 cells were grown on 20 mM glucose in 200 ml of SBM in a 2-L volume conical flask, washed in PBS and transferred into 2-L volume conical flasks that contained 380 ml each of SBM plus (1) phenanthrene or (2) phenanthrene and benzo[*a*]pyrene, 100 mg/L each (apparent solubility) in duplicates. Identically to as described above, at the start of incubation, PAHs were added, cell densities adjusted to 0.4 and cultures incubated for 14 days - however by rotary shaking - after which 30-ml volumes each of culture fluids were removed, transferred to 500-ml volume conical flasks, adjusted to pH 2 with HCl and extracted with 30-ml volumes of ethyl acetate by rotary shaking overnight in the dark at 4 °C at 200 rpm. Following, aqueous and organic phases were separated in 250-ml volume glass separatory funnels. Organic phases were passed through anhydrous sodium sulfate, concentrated by using a rotoevaporator under conditions as described above and the extracted materials were resuspended in 1 ml of methanol before analyses by liquid chromatography electrospray ionization tandem mass spectrometry (LC/ESI-MS/MS) analyses as described below.

1-Pyrenecarboxylic acid biotransformation assays

S. barthaii KK22 cells were grown in 20 ml of SBM in 100-ml volume conical flasks that contained 200 mg/L phenanthrene for 3 days after which cells were harvested by centrifugation (8700 × *g*, 10 min, 4 °C) and resuspended in SBM. Cells were transferred to 100-ml volume conical flasks that contained 20 ml of SBM plus 50 mg/L 1-pyrenecarboxylic acid that was applied in chloroform as described above (final OD_{600} = 0.2). Abiotic controls consisted of 50 mg/L of 1-pyrenecarboxylic acid without cells and biotic controls consisted of cells without 1-pyrenecarboxylic acid (OD_{600} = 0.2). All flasks were incubated by continuous rotary shaking at 150 rpm at 30 °C in the dark. Cultures were sampled at multiple times and were extracted with ethyl acetate as described above. Organic and aqueous phases were separated in glass separatory funnels, organic phases were collected after passing through anhydrous sodium sulfate, evaporated under a stream of filter-sterilized nitrogen gas and resuspended in methanol for analyses by LC/ESI-MS/MS.

Identification of PAH biotransformation products by LC/ESI(-)-MS(/MS) analyses of culture extracts

Unknown compounds extracted from *S. barthaii* KK22 cultures were analyzed by LC/ESI-MS(/MS) in full scan and product ion scan modes as described previously (Maeda et al., 2020). An analytical standard

Table 1
Recoveries of phenanthrene and benzo[*a*]pyrene (100 mg/L each) in biodegradation assays.

	Phenanthrene recovery[a] (%)		Benzo[*a*]pyrene recovery[a] (%)	
Time (days)	when cultured without benzo[*a*]pyrene	when cultured with benzo[*a*]pyrene	when cultured without phenanthrene	when cultured with phenanthrene
0	102.7 ± 2.2	97.8 ± 1.1	97.4 ± 2.0	101.8 ± 1.8
14	< 1.0[b]	< 1.0[b]	104.8 ± 1.0	77.6 ± 5.0

[a] Recoveries are expressed normalized against recoveries for the corresponding abiotic controls. [b] Not detected; values are expressed as the percent limit of detection under these conditions.

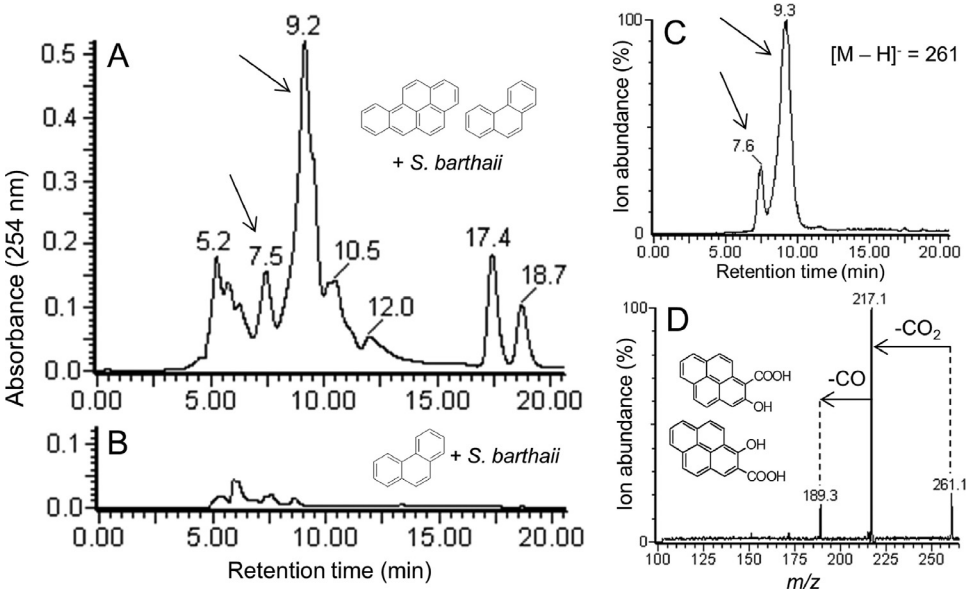

Fig. 1. Detection of chromatographically-separated biotransformation products extracted from cultures of *S. barthaii* KK22 cells exposed to benzo[*a*]pyrene and phenanthrene in the same culture (A) and *S. barthaii* KK22 cells exposed to phenanthrene without benzo[*a*]pyrene (B) after 14 days of incubation. (C) LC/ESI(-)-MS extracted ion chromatogram of unknown products that corresponded to $[M - H]^-$ = 261 from extracts of cultures of cells exposed to benzo[*a*]pyrene and phenanthrene. (D) LC/ESI(-)-MS/MS product ion scan mass spectrum ($[M - H]^-$ = 261) of the product that eluted at 7.6 min in (C). The baseline was magnified twenty-fold with the exception of the most abundant ion.

of 1-pyrenecarboxylic acid dissolved in methanol was analyzed under identical LC/ESI(-)-MS(/MS) conditions.

Results

Monitoring of phenanthrene and benzo[a]pyrene biodegradation by GC

S. barthaii KK22 cells were exposed separately to (i) phenanthrene, (ii) benzo[*a*]pyrene, or (iii) both phenanthrene and benzo[*a*]pyrene after which PAH concentrations in culture media were measured after 14 days. Results showed that phenanthrene was biodegraded to undetectable levels when cultured both with or without benzo[*a*]pyrene (reported as percent limit of detection in Table 1). Contrastively, benzo[*a*]pyrene biodegradation only occurred in the presence of phenanthrene *i.e.*, without phenanthrene, benzo[*a*]pyrene biodegradation was less than approximately 5% even when experimental error was considered (Table 1). In the presence of phenanthrene, approximately 20% of benzo[*a*]pyrene was removed whereby the average recovery was 77.6 ± 5.0% (Table 1) and this corresponded to a mass of approximately 1.1 mg of benzo[*a*]pyrene.

Detection and identification of abundant o-hydroxy-tetraaromatic acid biotransformation products

Considering that the results of quantitative analyses indicated that strain KK22 was capable of cometabolic benzo[*a*]pyrene biodegradation, qualitative analyses were conducted by LC/ESI-MS(/MS) coupled with UV detection to confirm quantitative analyses. Shown in Figs. 1A and 1B are the results of separation and detection (at 254 nm) of biotransformation products in organic extracts when *S. barthaii* KK22 cells were exposed to both phenanthrene and benzo[*a*]pyrene (Fig. 1A) and when cells were exposed only to phenanthrene (Fig. 1B). Comparison of these results showed that numerous peaks were detected when benzo[*a*]pyrene was present through approximately 20 min (Fig. 1A) that were either not detected or detected in relatively small amounts in extracts when benzo[*a*]pyrene was not (Fig. 1B). From these results it was concluded that peaks detected when benzo[*a*]pyrene was present may have represented benzo[*a*]pyrene biotransformation products (Fig. 1A; time course results are given in Fig. S1).

Next, results of LC-MS full scan analyses combined with mass selection techniques showed that two abundantly detected products eluted at retention times (t_R) of 7.6 and 9.3 min that each corresponded to the deprotonated molecule $[M - H]^-$ = 261 and the extracted ion chromatogram (EIC) for these unknown compounds is shown in Fig. 1C. These two products also corresponded to two products that were detected in relatively high concentration at 254 nm (designated by arrows in Fig. 1A). When EICs for $[M - H]^-$ = 261 were compared to other culture conditions (cells exposed to phenanthrene without benzo[*a*]pyrene and abiotic controls that consisted of phenanthrene and benzo[*a*]pyrene without cells) these products were not detected (data not shown). These results provided strong evidence that these unknown compounds were benzo[*a*]pyrene biotransformation products.

Product ion scan analyses of these products were conducted and results showed that nearly identical fragmentation patterns were observed for each compound (Fig. 1D and Table 2). The mass spectrum of the compound that eluted at 7.6 min is shown in Fig. 1D when it was produced under relatively strong CID conditions (20 eV). The most abundant ion, *m/z* 217, occurred through a loss of 44 Da from the parent deprotonated molecule as CO_2. The second diagnostic ion, *m/z* 189 represented losses of CO_2 and CO as 72 Da from the parent deprotonated molecule whereby carbonyl loss of 28 Da occurred through a hydroxyl moiety (Xu et al., 2004; Matsui et al., 2019). Considering these fragmentation patterns, molar masses of 262 Da each and molecular formulae of $C_{17}H_{10}O_3$, these products appeared to be two *o*-hydroxy-tetraaromatic acid products of benzo[*a*]pyrene biotransformation (Fig. 1D).

Table 2
Results of LC/ESI(-)-MS/MS product ion scan analyses of biotransformation products discussed in this report. Compounds are listed in the order that they are introduced in the Results section.

$[M-H]^-$	t_R[a] (min)	CID[b] (eV)	Diagnostic fragments [*m/z* (ion,% relative intensity)]	Identity assignment
261	7.6	20	261 (M^-, 1), 217 ($M^- - CO_2$, 100), 189 ($M^- - CO_2 - CO$, 1)	2-hydroxypyrene-1-carboxylic acid[c]
261	9.3	20	261 (M^-, 2), 217 ($M^- - CO_2$, 100), 189 ($M^- - CO_2 - CO$, 1)	1-hydroxypyrene-2-carboxylic acid
283	17.5	8	283 (M^-, 100), 265 ($M^- - H_2O$, 2), 255 ($M^- - CO$, <1), 251 ($M^- - C_{20}H_{11}^-$, 2), 247 ($M^- - 2H_2O$, 25), 239 ($C_{19}H_{11}^-$, 3), 227 ($M^- - 2CO$, 1)	7,8- or 9,10-dihydroxy-benzo[*a*]pyrene
283	18.7	8	283 (M^-, 100), 265 ($M^- - H_2O$, 1), 255 ($M^- - CO$, 3), 251 ($M^- - C_{20}H_{11}^-$, 1), 247 ($M^- - 2H_2O$, 5), 239 ($C_{19}H_{11}^-$, 3)	7,8- or 9,10-dihydroxy-benzo[*a*]pyrene
315	5.4	20	315 (M^-, 6), 297 ($M^- - H_2O$, <1), 271 ($M^- - CO_2$, 4), 227 ($M^- - 2CO_2$, 100), 201 ($C_{16}H_9^-$, 7)	1-(2-)(2-carboxyvinyl)pyrene-2-(1-)carboxylic acid
315	7.5	20	315 (M^-, 58), 297 ($M^- - H_2O$, 2), 287 ($M^- - CO$, 21), 271 ($M^- - CO_2$, 17), 253 ($M^- - CO_2 - H_2O$, 4), 243 ($M^- - CO_2 - CO$, 11), 227 ($C_{18}H_{11}^-$, 100), 201 ($C_{16}H_9^-$, 8)	4-[1-(2-)hydroxypyren-2-(1-)yl]-2-oxo-but-3-enoic acid
289	5.7	8	289 (M^-, 100), 245 ($M^- - CO_2$, 55), 201 ($M^- - CO_2$, 23)	pyrene-1,2-dicarboxylic acid
245	12.3	8	245 (M^-, 100), 201 ($M^- - CO_2$ / $C_{16}H_9^-$, 27)	1-(2-)pyrenecarboxylic acid
245	12.4	8	245 (M^-, 100), 201 ($M^- - CO_2$ / $C_{16}H_9^-$, 69)	1-pyrenecarboxylic acid authentic standard
265	4.5	8	265 (M^-, 100), 247 ($M^- - H_2O$, 14), 229 ($M^- - 2H_2O$, 36), 221 ($M^- - CO_2$, 11), 203 ($M^- - CO_2 - H_2O$, 3), 193 ($M^- - CO_2 - CO$, 15), 177 ($C_{14}H_9^-$, 4)	2-hydroxy-3-(9-oxophenalen-1-yl)prop-2-enoic acid / 3-(9-hydroxyphenalen-1-ylidene)-2-oxo-propanoic acid
293	7.9	20	293 (M^-, 3), 249 ($M^- - CO_2$, 42), 205 ($M^- - CO_2$, 100), 177 ($C_{14}H_9^-$, 18), 115 ($C_4H_3O_4^-$, 13)	2-[(9-oxophenalen-1-yl) methylene]propanedioic acid
261	7.7	20	261 (M^-, 5), 217 ($M^- - CO_2$, 100), 189 ($M^- - CO_2 - CO$, 1)	2-hydroxypyrene-1-carboxylic acid[c]
233	9.1	8	233 (M^-, 100), 215 ($M^- - H_2O$, 1), 201 ($C_{16}H_9^-$, 1) 189 ($C_{15}H_9^-$, 1) 177 ($C_{14}H_9^-$, 1)	1,2-dihydroxypyrene
223	4.1	20	223 (M^-, 26), 205 ($M^- - H_2O$, 52), 195 ($M^- - CO$, 15) 179 ($M^- - CO_2$, 100)	9-oxophenalene-1-carboxylic acid
195	5.2	20	195 (M^-, 21), 177 ($M^- - H_2O$, 100), 159 ($M^- - 2H_2O^-$, 4)	9-hydroxyphenalen-1-one

[a] t_R, retention time, EIC.
[b] Collision induced dissociation energy.
[c] Positions of hydroxyl and carboxyl moieties were confirmed through results of 1-pyrenecarboxylic acid biodegradation assays.

Related to these results, when bacterial biotransformation of the five-ring PAH benzo[*k*]fluoranthene (molar mass identical to benzo[*a*]pyrene; 252 Da) was examined previously, a single biotransformation product that possessed a molar mass of 262 Da was relatively strongly detected (Maeda et al., 2014). CID fragmentation of this compound revealed a spectrum that was nearly identical to the benzo[*a*]pyrene products detected herein that also corresponded to $[M-H]^- = 261$. The benzo[*k*]fluoranthene biotransformation product was identified as an *o*-hydroxy-tetraaromatic acid, 9-hydroxyfluoranthene-8-carboxylic acid that was produced through 8,9-carbon position oxidation of benzo[*k*]fluoranthene. Interestingly, dioxygenation of the exposed kata-annelated ring of benzo[*k*]fluoranthene may result in the production of only one downstream *o*-hydroxy-tetraaromatic acid product with a molar mass of 262 Da due to the molecular symmetry of the molecule, *i.e.*, 9-hydroxyfluoranthene-8-carboxylic acid. When considering the benzo[*a*]pyrene molecule however, a 7,8- or 9,10-carbon position oxidation of the exposed kata-annelated ring may result in two possible downstream constitutionally isomeric *o*-hydroxy-tetraaromatic acids with molar masses equal to 262 Da each. In this work, the two compounds that corresponded to $[M-H]^- = 261$ were proposed to be 2-hydroxypyrene-1-carboxylic acid and 1-hydroxypyrene-2-carboxylic acid (Fig. 1D).

In a previous benzo[*a*]pyrene biodegradation study (Rentz et al., 2008), LC-MS in full scan mode was used to detect a compound that corresponded to *m/z* 261 that was detected in experiments from media that contained 1.2 μg/L benzo[*a*]pyrene. Our understanding is that the detected peak was next correlated to an ion equal to *m/z* 217 by repeat analysis in full scan mode by using greater collision cell energy and from these data hydroxypyrene-carboxylic acids were proposed as potential biodegradation products; the organism was a reported as a *Sphingomonas* strain by 16S rRNA gene sequencing of 862 bases (Rentz et al., 2008).

Identification of upstream benzo[a]pyrene biotransformation products

As shown in Fig. 1A, two of the latest-eluted biotransformation products were detected at retention times of 17.4 and 18.7 min each (UV_{254nm}) and they were found to correspond to deprotonated molecules equal to $[M-H]^- = 283$ each. CID fragmentation of these compounds revealed fragmentation patterns that were similar to each other (Table 2). Results for the earlier-eluted compound (t_R = 17.4 min) are given in Fig. 2A whereby *m/z* 265 and *m/z* 247 represented losses of one or two water molecules respectively from the parent deprotonated molecule and formation of *m/z* 255 occurred through carbonyl loss of 28 Da from the parent deprotonated molecule. Detection of *m/z* 239 occurred through losses of a carbonyl and water to form a five-membered ring (Fig. 2A) and provided evidence for the presence of phenolic hydroxyl groups on the parent molecule. Interestingly, *m/z* 251 was also detected and appeared to represent the deprotonated benzo[*a*]pyrene molecule. Considering these fragmentation patterns, compounds with molar masses of 284 Da and molecular formulae of $C_{20}H_{12}O_2$, these compounds were assigned identities of 7,8- and 9,10-dihydroxy-benzo[*a*]pyrene (Table 2) and the structure for 9,10-dihydroxy-benzo[*a*]pyrene is given in Fig. 2A.

The two highest molar mass products that were revealed possessed identical deprotonated molecules of $[M-H]^- = 315$ each and retention times of approximately 5.4 and 7.5 min; they were subsequently investigated by CID (Figs. 2B and 2C). Results of CID analyses of the earlier-eluted compound (Fig. 2B) showed that three diagnostic ions were produced that revealed losses of 44 and 88 Da each from the parent deprotonated molecule (*m/z* 271 and *m/z* 227 respectively) including production of the strong diagnostic fragment, *m/z* 201 which represented the deprotonated pyrene molecule (Nourse et al., 1992). Loss of water as 18 Da from the parent deprotonated molecule was also detected (*m/z* 297). Considering these results, a molar mass of 316 Da and a molecular formula of $C_{20}H_{12}O_4$, this compound was proposed to be one of two possible intradiol cleavage products, 1-(2-carboxyvinyl)pyrene-2-carboxylic acid or 2-(2-carboxyvinyl)pyrene-1-carboxylic acid and the structure for 1-(2-carboxyvinyl)pyrene-2-carboxylic acid is given in Fig. 2B. These products may have occurred through *ortho* ring cleavage of upstream 7,8- and/or 9,10-dihydroxy-benzo[*a*]pyrene(s) identified above ($[M-H]^- = 283$ each).

CID analyses of the second unknown compound that corresponded to $[M-H]^- = 315$ revealed fragment *m/z* 287 which represented loss of 28 Da as CO from the parent deprotonated molecule and *m/z* 243 which represented loss of 72 Da from the parent deprotonated molecule as CO_2 and CO (Fig. 2C). Identically to its constitutional iso-

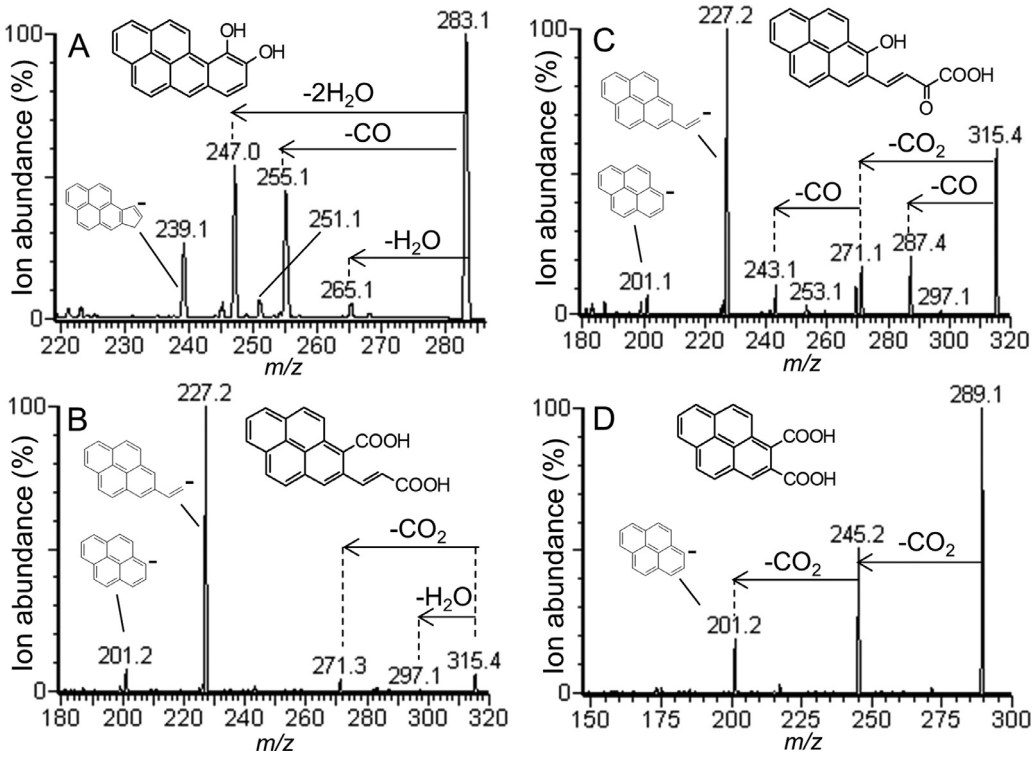

Fig. 2. LC/ESI(-)-MS/MS product ion scan mass spectra of the biotransformation products that corresponded to: (A) $[M - H]^-$ = 283, t_R = 17.5 min, (B) $[M - H]^-$ = 315, t_R = 5.4 min, (C) $[M - H]^-$ = 315, t_R = 7.5 min and (D) $[M - H]^-$ = 289, t_R = 5.7 min. The baseline in (A) was magnified 15-fold with the exception of the parent deprotonated molecule.

mer described above, the strong diagnostic fragment *m/z* 201 was detected as deprotonated pyrene in addition to *m/z* 297, *m/z* 271 and *m/z* 227 (Fig. 2C). This fragmentation pattern provided evidence that both CO and CO_2 were directly eliminated from the parent deprotonated molecule. Therefore, considering a molar mass of 316 Da and a molecular formula of $C_{20}H_{12}O_4$, these results supported that this compound was one of two potential extradiol cleavage products, 4-(1-hydroxypyren-2-yl)-2-oxo-but-3-enoic acid or 4-(2-hydroxypyren-1-yl)-2-oxo-but-3-enoic acid; 4-(1-hydroxypyren-2-yl)-2-oxo-but-3-enoic acid is shown in Fig. 2C. Such products may be formed through *meta* ring cleavage of upstream 7,8- and/or 9,10-dihydroxy-benzo[*a*]pyrene(s).

Results of product ion scan analyses of a biotransformation product that corresponded to $[M - H]^-$ = 289 (t_R = 5.7 min) revealed a simple mass spectrum that consisted of two abundant fragments (Fig. 2D) whereby again deprotonated pyrene was detected (*m/z* 201) which represented a loss of 88 Da ($2CO_2$) and *m/z* 245 was detected which represented a loss of 44 Da (CO_2) from the parent deprotonated molecule. Considering this fragmentation pattern, a molar mass of 290 Da, and a molecular formula of $C_{18}H_{10}O_4$, this compound was identified as pyrene-1,2-dicarboxylic acid. In conjunction with detection of carboxyvinyl-pyrene-carboxylic acids described above ($[M - H]^-$ = 315; t_R = 7.6 min; Fig. 2B) detection of pyrene-1,2-dicarboxylic acid provided further evidence for upstream *ortho*-cleavage events during benzo[*a*]pyrene biotransformation by this strain.

Detection, identification and confirmation of 1-pyrenecarboxylic acid as a product of benzo[a]pyrene biodegradation

Results of analysis of a relatively late-eluted compound (t_R = 12.3 min) that corresponded to $[M - H]^-$ = 245 is given in Fig. 3A (EIC) and 3B (CID) whereby a single loss of 44 Da as CO_2 from the parent deprotonated molecule to yield deprotonated pyrene (*m/z* 201) was revealed. Considering a molar mass of 246 Da, this simple mass spectrum and a molecular formula of $C_{17}H_{10}O_2$, this compound was proposed to be either 1-pyrene- and/or 2-pyrenecarboxylic acid(s).

1-Pyrenecarboxylic acid was commercially available and analysis of an authentic analytical standard of this compound in methanol revealed a nearly identical retention time and fragmentation pattern (Figs. 3C and 3D) when compared to the product detected in benzo[*a*]pyrene biodegradation extracts thereby confirming its production during benzo[*a*]pyrene biodegradation.

Detection and identification of downstream phenalenone biotransformation products

Fig. 4A shows CID results of a product that corresponded to [M – H]- = 265, t_R = 4.7 min. In addition to loss of water from the parent deprotonated molecule (*m/z* 247) there were direct losses of 28 Da as CO (*m/z* 237), 44 Da as CO_2 (*m/z* 221) and consecutive losses of 44 and 28 Da as CO_2 and CO, respectively (*m/z* 193). At the same time, the diagnostic ion, *m/z* 177 was detected which represented deprotonated 1-methylenephenalene (Fig. 4A). Taken together with a molar mass of 266 Da and a molecular formula of $C_{16}H_{10}O_4$, these data provided evidence that this compound was a three-ring PAH biotransformation product derived from a 1*H*-phenalene base and 2-hydroxy-3-(9-oxophenalen-1-yl)-prop-2-enoic acid is shown in Fig. 4A. This type of product may be formed through *meta* cleavage of 1,2-dihydroxy-pyrene for example.

A relatively high molar mass phenalenone product that corresponded to [M – H]- = 293 was also detected and CID analyses revealed consecutive losses of CO_2 as 44 and 88 Da each from the parent deprotonated molecule (*m/z* 249 and *m/z* 205, respectively; Fig. 4B). Again, the diagnostic fragment, deprotonated 1-methylenephenalene was also detected (*m/z* 177) and *m/z* 115 which represented deprotonated 2-methylenepropanedioic acid (Fig. 4B). Considering this fragmentation pattern, a molar mass of 294 Da and a molecular formula of $C_{17}H_{10}O_5$ this compound was proposed to be 2-(9-oxophenalen-1-yl)methylenepropanedioic acid as shown in Fig. 4B.

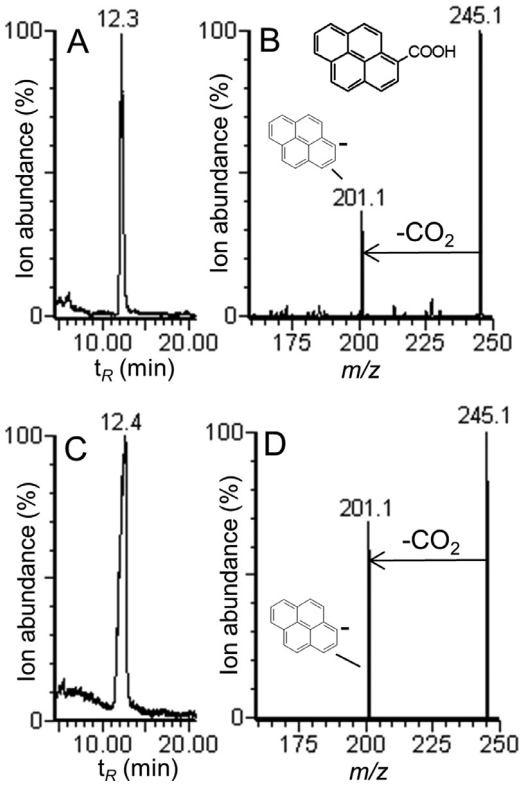

Fig. 3. (A) Extracted ion chromatogram of the unknown product that corresponded to $[M - H]^-$ = 245. (B) LC/ESI(-)-MS/MS product ion scan mass spectrum of the product in (A), $[M - H]^-$ = 245. (C) Extracted ion chromatogram of an authentic standard of 1-pyrenecarboxylic acid. (D) LC/ESI(-)-MS/MS product ion scan mass spectrum of an authentic standard of 1-pyrenecarboxylic acid, $[M - H]^-$ = 245.

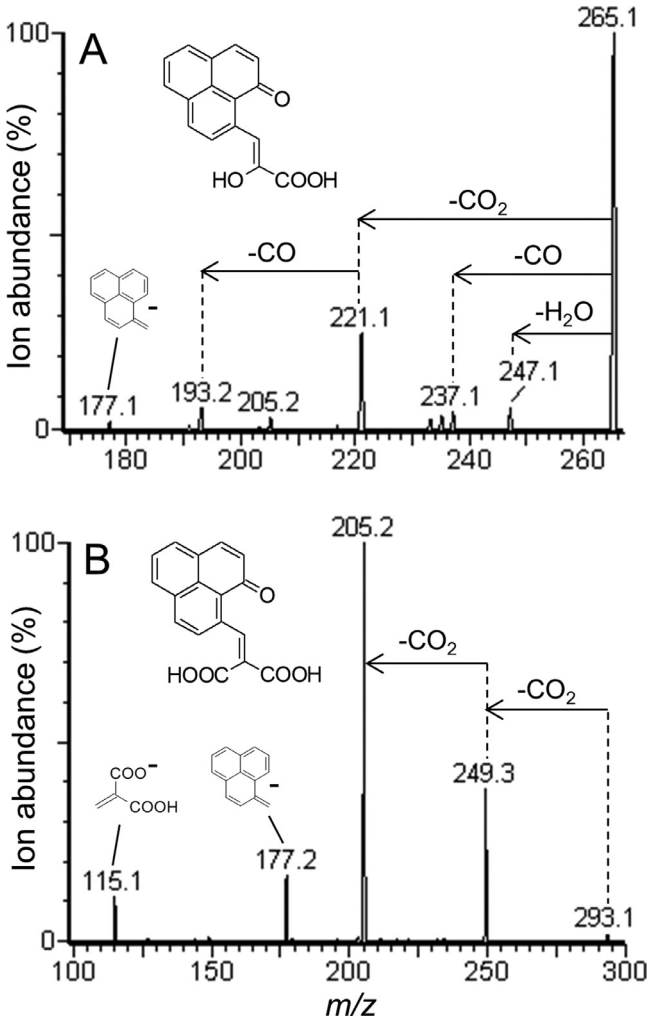

Fig. 4. LC/ESI(-)-MS/MS product ion scan mass spectra of the product that corresponded to $[M - H]^-$ = 265 (A) and the product that corresponded to $[M - H]^-$ = 293 (B). Except for the parent deprotonated molecule, the baseline in (A) was magnified ten-fold.

Identification of 2-hydroxypyrene-1-carboxylic acid, $[M - H]^-$ = 261, and products downstream from 1-pyrenecarboxylic acid

Following the confirmation that at least 1-pyrenecarboxylic acid was a product of benzo[*a*]pyrene biodegradation, 1-pyrenecarboxylic acid biotransformation assays were conducted using strain KK22 to determine if downstream products could be identified. Interestingly, a single peak that corresponded to the deprotonated molecule $[M - H]^-$ = 261 was strongly detected within 24 h and it eluted at a retention time of 7.7 min (Fig. 5A). This product possessed an identical deprotonated molecule value and a nearly identical retention time to a benzo[*a*]pyrene biotransformation product introduced in Fig. 1C. CID analysis of the pyrene-1-carboxylic acid product also revealed a nearly identical mass spectrum to the two benzo[*a*]pyrene products that corresponded to $[M - H]^-$ = 261 (Fig. 5B and Table 2) whereby the most abundant ion, *m/z* 217, occurred through a loss of CO_2 as 44 Da from the parent deprotonated molecule and *m/z* 189 represented losses of CO_2 and CO as 72 Da. Considering this fragmentation pattern, a molar mass of 262 Da, a molecular formula of $C_{17}H_{10}O_3$, and that this product was produced from 1-pyrenecarboxylic acid, it was assigned an identity of 2-hydroxypyrene-1-carboxylic acid. Identification of this product also therefore allowed for the differentiation of the two previously detected benzo[*a*]pyrene products that corresponded to $[M - H]^-$ = 261 whereby 2-hydroxypyrene-1-carboxylic acid was identified as the compound that eluted at 7.6 min (Fig. 1C).

A relatively late-eluting product that corresponded to a deprotonated molecule of $[M - H]^-$ = 233 (Fig. 5C) was detected at 9.1 min in 1-pyrenecarboxylic acid biodegradation assays and results of CID analysis revealed two strong diagnostic fragments, *m/z* 201 and *m/z* 177 which represented deprotonated pyrene and 1-methylenephenalene molecules, respectively. Also considering losses of water (*m/z* 215) and consecutive losses of water and carbonyl (*m/z* 189; Fig. 5C) combined with a molar mass of 234 Da and a molecular formula of $C_{16}H_{10}O_2$, this compound was proposed to be 1,2-dihydroxypyrene. Detection of 1,2-dihydroxypyrene from 1-pyrenecarboxylic acid was unexpected and its identification was of strong utility for constructing the benzo[*a*]pyrene biodegradation pathways described below.

Finally, Fig. 5D and E show CID results of two products that corresponded to $[M - H]^-$ = 223, t_R = 4.1 min and $[M - H]^-$ = 195, t_R = 5.2 min whereby it was revealed that these were phenalenone-derived compounds proposed to be 9-oxophenalene-1-carboxylic acid and 9-hydroxyphenalen-1-one, respectively. Results of LC analyses from 1-pyrenecarboxylic acid biotransformation assays are given in Fig. S2.

Construction of a benzo[a]pyrene biotransformation pathway for sphingomonads

Based upon the results of these analyses, pathways for the cometabolic biodegradation of benzo[*a*]pyrene by *S. barthaii* KK22 were constructed and are presented in Fig. 6. Initial oxidation of the benzo[*a*]pyrene molecule at the 7,8- and 9,10-carbon positions occurred to produce benzo[*a*]pyrene-dihydrodiols that were reduced to their respective dihydroxy-benzo[*a*]pyrenes. These PAH-catechols were de-

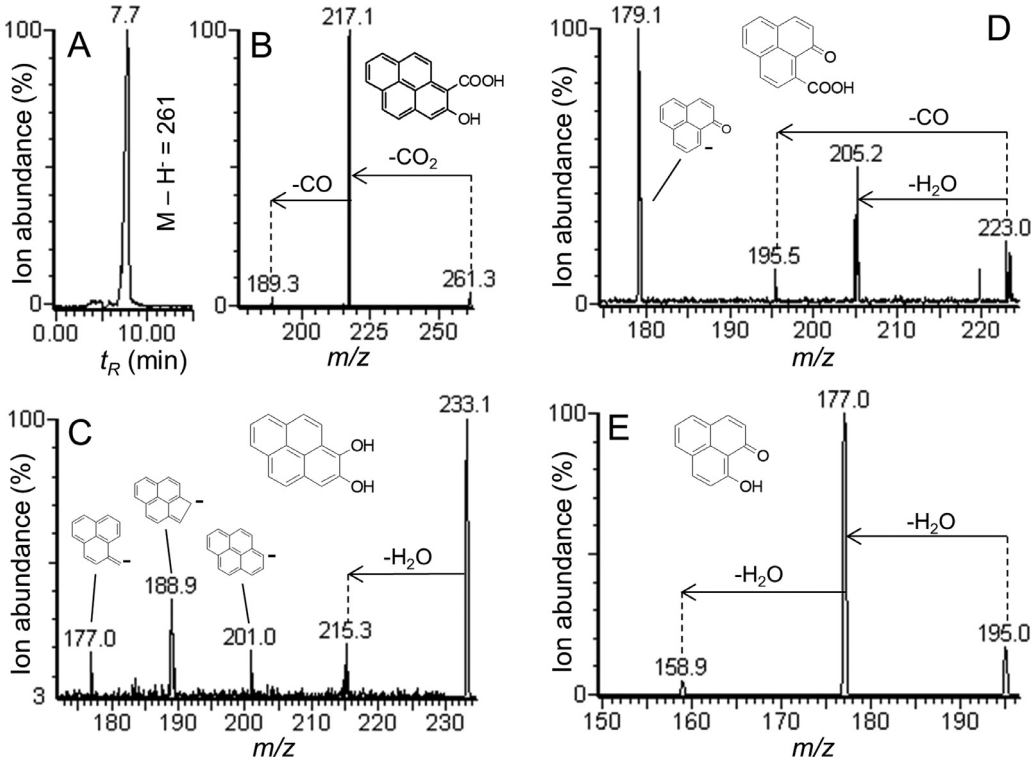

Fig. 5. (A) Extracted ion chromatogram of a 1-pyrenecarboxylic acid biotransformation product that corresponded to $[M - H]^-$ = 261. LC/ESI(-)-MS/MS product ion scan mass spectra of 1-pyrenecarboxylic acid biotransformation products that corresponded to $[M - H]^-$ = 261 (B), $[M - H]^-$ = 233 (C), $[M - H]^-$ = 223 (D) and $[M - H]^-$ = 195 (E). Except for the parent deprotonated molecule, the baseline in (B) was magnified 40-fold and the baseline in (D) was magnified 30-fold.

tected as the latest-eluted products that corresponded to $[M - H]^-$ = 283 each (Fig. 1A) and were subjected to ring fission by both intradiol and extradiol ring cleavage events to produce tetraaromatic products that corresponded to $[M - H]^-$ = 315: 1(2)-(2-carboxyvinyl)pyrene-2(1)-carboxylic acid(s) and 4-[1(2)-hydroxypyren-2(1)-yl]-2-oxo-but-3-enoic acid(s) respectively (Fig. 2B and C). Production of carboxyvinyl intradiol PAH cleavage products is less common and has been shown before for 2- and 3-ring PAHs (Seo et al., 2006, 2007; Fukuoka et al., 2015) but not for benzo[*a*]pyrene. Pyrene-1,2-dicarboxylic acid, $[M - H]^-$ = 289, was detected and confirmed that intradiol cleavage had occurred because this product may only be produced downstream from carboxyvinylpyrene-carboxylic acids (Fig. 6). Similarly, pyrenecarboxylic acids ($[M - H]^-$ = 245) were likely produced from upstream extradiol cleavage products (analogous compounds were detected by Schneider et al., 1996) and transformed into the consistently most abundantly detected products that corresponded to $[M - H]^-$ = 261, the hydroxypyrene-carboxylic acids (Fig. 6) enroute to 1,2-dihydroxypyrene or ring-opened products. At the same time, pyrenecarboxylic acids were transformed into 1,2-dihydroxypyrene through 1,2-dihydroxypyrene-carboxylic acid intermediates as shown in Fig. 6. These oxidation steps may be based upon the same mechanism of arene-diol generation from benzoic acid dioxygenation enroute to catechol that has been shown to occur in this strain and other strains (Sun et al., 2008; Maeda et al., 2020). Pathway convergence appeared to occur through production of 1,2-dihydroxypyrene ($[M - H]^-$ = 233) from pyrene-1,2-carboxylic acid and hydroxypyrene-carboxylic acids (Fig. 6). Three-ring phenalenone products were detected and indicated that downstream transformation had continued through extradiol cleavage of 1,2-dihydroxypyrene. At the same time, production of the phenalenone derivative, 2-[(9-oxophenalen-1-yl)methylene]-propanedioic acid, $[M - H]^-$ = 293, may only have occurred through direct ring-opening of 1-hydroxypyrene-2-carboxylic acid ultimately leading to potential pathway convergence through 9-oxophenalene-1-carboxyclic acid and 9-hydroxy-phenalen-1-one. Interestingly, this mechanism of ring opening (Fig. 6) was recently shown in a *Sphingobium* species (Roy et al., 2012) whereby *Sphingobium* sp. strain PNB directly cleaved hydroxy-naphthoic acid intermediates of phenanthrene biodegradation to compounds that were structurally analogous to [(9-oxophenalen-1-yl)methylene]-propanedioic acid (Roy et al., 2012).

Discussion

S. barthaii KK22 grew on phenanthrene as a sole source of carbon and energy but was unable to biotransform benzo[*a*]pyrene in the absence of phenanthrene and it was therefore concluded that benzo[*a*]pyrene biotransformation occurred through cometabolism. Initial oxidation of the benzo[*a*]pyrene molecule by bacterial dioxygenases may hypothetically occur in at least six different locations, i.e., oxidation at the 1,2-, 2,3-, 4,5-, 7,8-, 9,10-,and/or 11,12-carbon positions and depending upon the location of the initial oxidation event, the structures of downstream products shall vary (Kweon et al., 2011). Herein, such information was useful to determine the positions of initial oxidation on the benzo[*a*]pyrene molecule and for construction of biotransformation pathways. For example, 1-pyrenecarboxylic acid was identified in culture extracts as a benzo[*a*]pyrene biodegradation product and in conjunction with other identified products, provided key supportive evidence that initial oxidation occurred on the kata-annelated ring of benzo[*a*]pyrene; precisely, at the 7,8-carbon positions of benzo[*a*]pyrene. At the same time, identification of both 2-hydroxypyrene-1-carboxylic acid and 1-hydroxypyrene-2-carboxylic acid provided strong evidence that again the kata-annelated ring of benzo[*a*]pyrene was biotransformed through initial oxidations at the 7,8- and 9,10-carbon positions of benzo[*a*]pyrene.

During aerobic PAH biodegradation, formation of a *cis*-dihydrodiol is considered to be the critical first step (Fu et al., 2018). Herein, initial dioxygenation yielded benzo[*a*]pyrene-dihydrodiols followed by dehy-

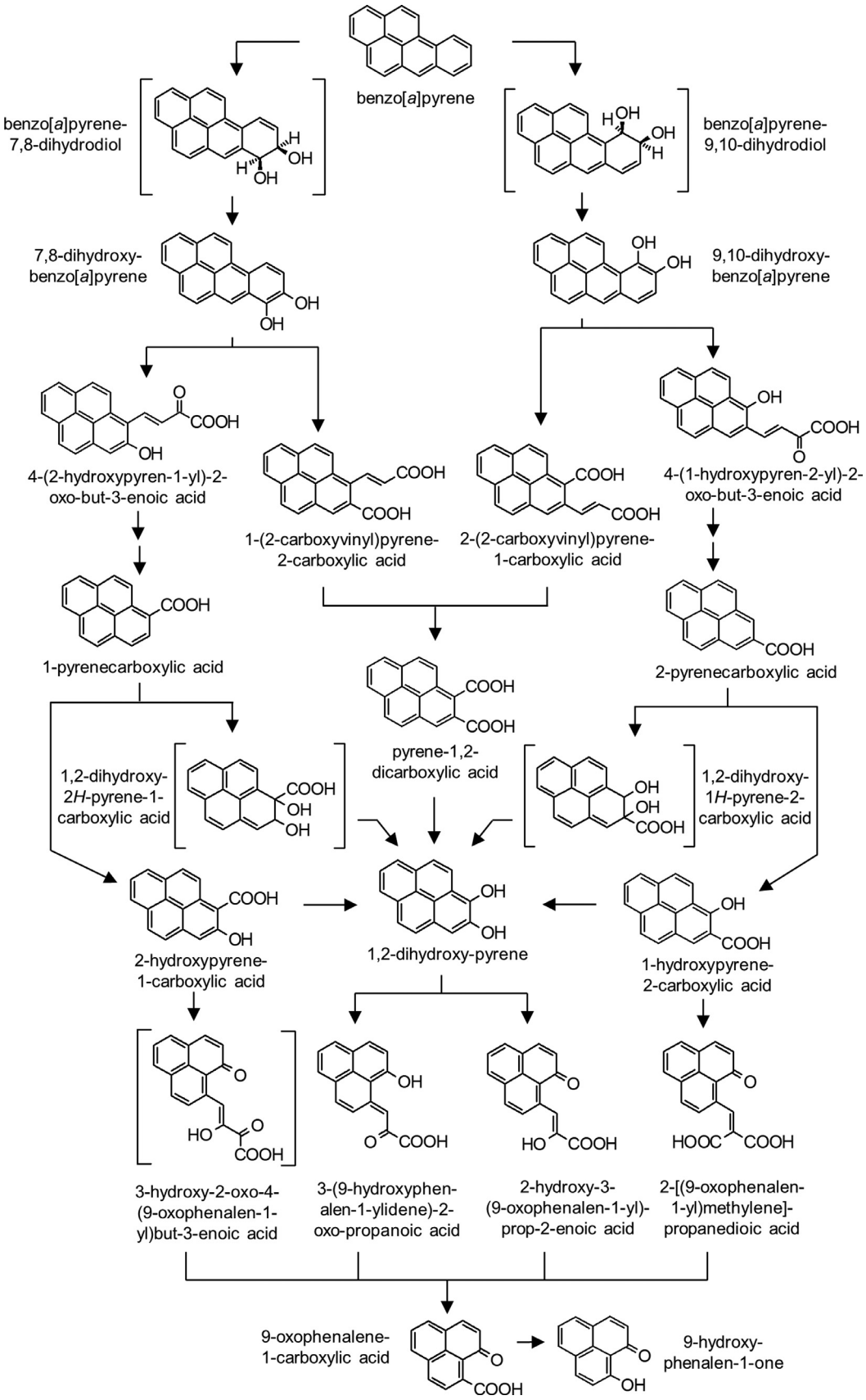

Fig. 6. Pathways proposed for the cometabolic biodegradation of benzo[*a*]pyrene by *Sphingobium barthaii* KK22. Compounds in brackets are proposed intermediates.

drogenase reduction to form 7,8- and 9,10-dihydroxy-benzo[*a*]pyrene. Previously, the three protein components of a biphenyl-2,3-dioxygenase system that encoded for the genes *bphA4, bphA3* and *bphA1fA2f* from *Sphingobium yanoikuyae* strain B1 were shown to facilitate the dioxygenation of benzo[*a*]pyrene to *cis*-7,8- and *cis*-9,10-dihydrodiols by expression in *E. coli* but not at other positions on the pericondensed rings (Ni Chadhian et al., 2007; Yu et al., 2007). In the case of strain KK22, different investigations showed that there were at least seven sets of aromatic ring-hydroxylating oxygenases (RHOs) in its genome (Maeda et al., 2013; Maeda et al., 2014; Mori and Kanaly, 2020, 2021) and among these RHOs greater than 94% amino acid identity of the concatenated sequences was revealed when compared to *bphA1fA2f* homologues in *S. yanoikuyae* B1 (Maeda et al., 2020). Contrastively, strain KK22 also appeared unable to biotransform the 4-ring pericondensed PAH pyrene similarly to strain B1 (unpublished results). These findings were in-line with results of investigations involving the PAH dioxygenase system of HMW PAH-degrading *Sphingomonas* sp. strain CHY-1 (*PhnA4, PhnA3 and PhnI*) where it was found that pyrene was also not a good substrate (Demaneche et al., 2004; Jouanneau et al., 2016). However, identically to strain KK22, oxidation of only the kata-annelated ring of benzo[*a*]pyrene was shown to occur by strain CHY-1 whereby at least 9,10-dihydrodiols were identified (Demaneche et al., 2004; Jouanneau et al., 2016). Through molecular modeling studies, it was reported that a large hydrophobic substrate binding cavity was necessary to accommodate the 5-ring benzo[*a*]pyrene molecule in strain CHY-1 (Jakoncic et al., 2007), *Sphingobium* sp. strain FB3 (Fu et al., 2018) and *Sphingobium* sp. strain PNB (Khara et al., 2014, 2018).

Aromatic ring-opening of the kata-annelated ring by strain KK22 occurred by extradiol and intradiol cleavage to produce hydroxypyrene-oxobutenoic acids and carboxyvinylpyrene-carboxylic acids, respectively (Fig. 6). Extradiol ring-opened products of benzo[*a*]pyrene through the 7,8-carbon positions (Schneider et al., 1996) and 9,10-carbon positions (Schneider et al., 1996; Moody et al., 2004) were identified from *Mycobacterium* spp. before, however, intradiol cleavage products of benzo[*a*]pyrene through the kata-annelated ring have not been reported. At the same time, the extradiol ring-cleavage product of the kata-annelated ring of benzo[*a*]pyrene, hydroxypyrene-oxobutenoic acid (316 Da) was identified for the first time from a Gram-negative organism. Pyrene-1,2-carboxylic acid was also identified in culture media and provided further evidence that intradiol biotransformation mechanisms were active.

Interestingly, 2-hydroxypyrene-1-carboxylic acid was detected as a biotransformation product of 1-pyrenecarboxylic acid and this supported that hydroxypyrene-carboxylic acids were downstream products of pyrenecarboxylic acids metabolism during benzo[*a*]pyrene catabolism (Fig. 6). Alternatively, pyrenecarboxylic acids were potentially transformed into arene-diols through 1,2-dihydroxy-2(1)*H*-pyrene-1(2)-carboxylic acids (Fig. 6). Hydroxypyrene-carboxylic acids may be acted upon by gene products of the *ahdA1*[*c-e*]*A2*[*c-e*] RHOs to again produce 1,2-dihydroxy-pyrene by decarboxylation (Pinyakong et al., 2003) or through direct oxidation and ring fission to produce three-ring phenalenone products; the latter through a dioxygenation mechanism that has recently been shown to occur during PAH biodegradation in *Sphingobium* (Roy et al., 2012) and *Staphylococcus* spp. (Mallick et al., 2007). Three RHOs responsible for the conversion of salicylic acids to catechols that were characterized in *Sphingobium* sp. strain P2, AhdA1[c-e]A2[c-e], (Pinyakong et al., 2003) were found to share amino acid identities of 99.5%, 98.2% and 97.1% respectively with strain KK22 AhdA1[c-e]A2[c-e] homologues. These enzymes were reported to be inactive against two-ring hydroxy-naphthoic acids (Pinyakong et al., 2003). Still, little is known in regard to the enzymes involved in many downstream PAH biotransformation steps (Zhao et al., 2017). At the same time, the gene(s) responsible for direct ring-opening of hydroxy-naphthoic acids during phenanthrene biodegradation are also unknown (Roy et al., 2012). MS results herein supported that at least four three-ring compounds appeared in culture extracts, likely as phenalenone products. Phenalenones such as 9-hydroxy-phenalen-1-one were identified as products of pyrene biodegradation, however the greater molar mass products described above were not (Heitkamp et al., 1988).

Sphingomonads have been reported to biotransform many different types of organic pollutants including PAHs (Baboshin et al., 2008; Stolz, 2009; Aylward et al., 2013; Stolz, 2014) and it has been discussed that they survive and may thrive in contaminated soil environments due to their abilities to withstand potentially high amounts of organic pollutant and metals contamination in soils (Cunliffe et al., 2006; Cunliffe and Kertesz, 2006; Kanaly et al., 2015; Chen et al., 2016; Mahbub et al., 2016; Volpicella et al., 2017). Herein it was demonstrated that although strain KK22 was able to biotransform benzo[*a*]pyrene including ring-opening, it required an additional carbon source for growth. These results indicate that benzo[*a*]pyrene biodegradation in the environment likely requires cometabolism in addition to the cooperation of other bacterial members to facilitate efficient biodegradation of downstream products. In the soil environment where many different types of organisms are present, including actinomycete mycobacteria, interspecies cooperation may facilitate biodegradation of 4- and 3-ring benzo[*a*]pyrene products as carbon sources (Schneider et al., 1996; Moody et al., 2004; Kweon et al., 2011).

Conclusions

Past work by many research groups over the years have indicated that biotransformation of benzo[*a*]pyrene by bacteria occurs by cometabolic metabolism and the results of this study continued to support this hypothesis. At the same time, through a combination of comparative biodegradation assays and comprehensive CID analyses, the identities of thirteen benzo[*a*]pyrene biotransformation products were proposed, some of them novel, and benzo[*a*]pyrene biotransformation pathways were constructed. These pathways differed from previously constructed pathways. Overall, our understanding of the manner by which bacteria and specifically members of the genus *Sphingobium* may biotransform HMW PAHs such as benzo[*a*]pyrene was expanded in conjunction with demonstration of the utility of LC/ESI-MS/MS to elucidate hazardous pollutant biodegradation mechanisms.

Declaration of Competing Interest

The authors declare that they have no known competing financial interests or personal relationships that could have appeared to influence the work reported in this paper.

Acknowledgments

This work was supported in part by the Japan Society for the Promotion of Science (JSPS) KAKENHI grant 17K00555 and 26505010 to R.A.K and grant 19K15738 to J.F.M.

Supplementary materials

Supplementary material associated with this article can be found, in the online version, at doi:10.1016/j.hazadv.2021.100018.

References

Atlas, R.M., 1993. Handbook of Microbiological Media. CRC Press, BocaRaton, FL.
Aylward, F.O., McDonald, B.R., Adams, S.M., Valenzuela, A., Schmidt, R.A., Goodwin, L.A., Woyke, T., Currie, C.R., Suen, G., Poulsen, M., 2013. Comparison of 26 sphingomonad genomes reveals diverse environmental adaptations and biodegradative capabilities. Appl. Environ. Microbiol. 79, 3724–3733.
Baboshin, M., Akimov, V., Baskunov, B., Born, T.L., Khan, S.U., Golovleva, L., 2008. Conversion of polycyclic aromatic hydrocarbons by *Sphingomonas* sp. VKM B-2434. Biodegradation 19, 567–576.

Chen, C., Lei, W., Lu, M., Zhang, J., Zhang, Z., Luo, C., Chen, Y., Hong, Q., Shen, Z., 2016. Characterization of Cu (II) and Cd (II) resistance mechanisms in *Sphingobium* sp. PHE-SPH and *Ochrobactrum* sp. PHE-OCH and their potential application in the bioremediation of heavy metal-phenanthrene co-contaminated sites. Environ. Sci. Pollut. Res. 23, 6861–6872.

Cunliffe, M., Kawasaki, A., Fellows, E., Kertesz, M.A., 2006. Effect of inoculum pretreatment on survival, activity and catabolic gene expression of *Sphingobium yanoikuyae* B1 in an aged polycyclic aromatic hydrocarbon-contaminated soil. FEMS Microbiol. Ecol. 58, 364–372.

Cunliffe, M., Kertesz, M.A., 2006. Autecological properties of soil sphingomonads involved in the degradation of polycyclic aromatic hydrocarbons. Appl. Microbiol. Biotechnol. 72, 1083–1089.

Demaneche, S., Meyer, C., Micoud, J., Louwagie, M., Willison, J.C., Jouanneau, Y., 2004. Identification and functional analysis of two aromatic-ring-hydroxylating dioxygenases from a *Sphingomonas* strain that degrades various polycyclic aromatic hydrocarbons. Appl. Environ. Microbiol. 70, 6714–6725.

Fernández-Luqueño, F., Valenzuela-Encinas, C., Marsch, R., Martínez-Suárez, C., Vázquez-Núñez, E., Dendooven, L., 2011. Microbial communities to mitigate contamination of PAHs in soil - possibilities and challenges: a review. Environ. Sci. Pollut. Res. 18, 12–30.

Folwell, B.D., McGenity, T.J., Whitby, C., 2016. Biofilm and planktonic bacterial and fungal communities transforming high-molecular-weight polycyclic aromatic hydrocarbons. Appl. Environ. Microbiol. 82, 2288–2299.

Fu, B., Li, Q.X., Xu, T., Cui, Z.L., Sun, Y., Li, J., 2014. *Sphingobium* sp. FB3 degrades a mixture of polycyclic aromatic hydrocarbons. Int. Biodeterior. Biodegradation 87, 44–51.

Fu, B., Xu, T., Cui, Z., Ng, H.L., Wang, K., Li, J., Li, Q.X., 2018. Mutation of phenylalanine-223 to leucine enhances transformation of benzo[*a*]pyrene by ring-hydroxylating dioxygenase of *Sphingobium* sp. FB3 by increasing accessibility of the catalytic site. J. Agric. Food Chem. 66, 1206–1213.

Fukuoka, K., Tanaka, K., Ozeki, Y., Kanaly, R.A., 2015. Biotransformation of indole by *Cupriavidus* sp. strain KK10 proceeds through *N*-heterocyclic-and carbocyclic-aromatic ring cleavage and production of indigoids. Int. Biodeterior. Biodegradation 97, 13–24.

Frank, E.G., Sayer, J.M., Kroth, H., Ohashi, E., Ohmori, H., Jerina, D.M., Woodgate, R., 2002. Translesion replication of benzo[*a*]pyrene and benzo[*c*]phenanthrene diol epoxide adducts of deoxyadenosine and deoxyguanosine by human DNA polymerase *ι*. Nucleic Acids Res. 30, 5284–5292.

Gibson, D.T., Mahadevan, V., Jerina, D.M., Yogi, H., Yeh, H.J., 1975. Oxidation of the carcinogens benzo[*a*]pyrene and benzo[*a*]anthracene to dihydrodiols by a bacterium. Science 189, 295–297.

Goto, S., Mineki, S., Sugita, K., Endo, O., Murayama, R., Uchiyama, I., Tanaka, M., Hayakawa, K., 1997. Mutagenicity and PAH contents of the heavy oil that drifted ashore on the coast from the tanker Nakhodka. J. Environ. Chem. 7, 553–559.

Haritash, A.K., Kaushik, C.P., 2009. Biodegradation aspects of polycyclic aromatic hydrocarbons (PAHs): a review. J. Hazard. Mater. 169, 1–15.

Heitkamp, M.A., Freeman, J.P., Miller, D.W., Cerniglia, C.E., 1988. Pyrene degradation by a *Mycobacterium* sp.: identification of ring oxidation and ring fission products. Appl. Environ. Microbiol. 54, 2556.

Jakoncic, J., Jouanneau, Y., Meyer, C., Stojanoff, V., 2007. The catalytic pocket of the ring-hydroxylating dioxygenase from *Sphingomonas* CHY-1. Biochem. Biophys. Res. Commun. 352 (4), 861–866.

Jouanneau, Y., Meyer, C., Duraffourg, N., 2016. Dihydroxylation of four- and five-ring aromatic hydrocarbons by the naphthalene dioxygenase from *Sphingomonas* CHY-1. Appl. Microbiol. Biotechnol. 100, 1253–1263.

Juhasz, A.L., Naidu, R., 2000. Bioremediation of high molecular weight polycyclic aromatic hydrocarbons: a review of the microbial degradation of benzo[*a*]pyrene. Int. Biodeterior. Biodegradation 45, 57–88.

Kanaly, R., Bartha, R., Fogel, S., Findlay, M., 1997. Biodegradation of [^{14}C] benzo[*a*]pyrene added in crude oil to uncontaminated soil. Appl. Environ. Microbiol. 63, 4511–4515.

Kanaly, R.A., Bartha, R., Watanabe, K., Harayama, S., 2000. Rapid mineralization of benzo[*a*]pyrene by a microbial consortium growing on diesel fuel. Appl. Environ. Microbiol. 66, 4205–4211.

Kanaly, R.A., Bartha, R., Watanabe, K., Harayama, S., 2001. Enhanced mineralization of benzo[*a*]pyrene in the presence of nonaqueous phase liquids. Environ. Toxicol. Chem. 20, 498–501.

Kanaly, R.A., Harayama, S., 2000. Biodegradation of high-molecular-weight polycyclic aromatic hydrocarbons by bacteria. J. Bacteriol. 182, 2059–2067.

Kanaly, R.A., Harayama, S., 2010. Advances in the field of high-molecular-weight polycyclic aromatic hydrocarbon biodegradation by bacteria. Microb. Biotechnol. 3, 136–164.

Kanaly, R.A., Micheletto, R., Matsuda, T., Utsuno, Y., Ozeki, Y., Hamamura, N., 2015. Application of DNA adductomics to soil bacterium *Sphingobium* sp. strain KK22. Microbiologyopen 4, 841–856.

Kanaly, R.A., Watanabe, K., 2004. Multiple mechanisms contribute to the biodegradation of benzo[*a*]pyrene by petroleum-derived multicomponent nonaqueous-phase liquids. Environ. Toxicol. Chem. 23, 850–856.

Khara, P., Roy, M., Chakraborty, J., Ghosal, D., Dutta, T.K., 2014. Functional characterization of diverse ring-hydroxylating oxygenases and induction of complex aromatic catabolic gene clusters in *Sphingobium* sp. PNB. FEBS Open Bio 4, 290–300.

Khara, P., Roy, M., Chakraborty, J., Dutta, A., Dutta, T.K., 2018. Characterization of a topologically unique oxygenase from *Sphingobium* sp. PNB capable of catalyzing a broad spectrum of aromatics. Enzyme Microb. Technol. 111, 74–80.

Kriipsalu, M., Marques, M., Hogland, W., Nammari, D.R., 2008. Fate of polycyclic aromatic hydrocarbons during composting of oily sludge. Environ Technol 29, 43–53.

Kunihiro, M., Ozeki, Y., Nogi, Y., Hamamura, N., Kanaly, R.A., 2013. Benz[*a*]anthracene biotransformation and production of ring fission products by *Sphingobium* sp. strain KK22. Appl. Environ. Microbiol. 79, 4410–4420.

Kweon, O., Kim, S.J., Holland, R.D., Chen, H., Kim, D.W., Gao, Y., Yu, L.-.R., Baek, S., Baek, D.-.H., Ahn, H., Cerniglia, C.E., 2011. Polycyclic aromatic hydrocarbon metabolic network in *Mycobacterium vanbaalenii* PYR-1. J. Bacteriol. 193, 4326.

Leon, V., Kumar, M., 2005. Biological upgrading of heavy crude oil. Biotechnol. Bioprocess Eng. 10, 471–481.

Lundstedt, S., White, P.A., Lemieux, C.L., Lynes, K.D., Lambert, I.B., Öberg, L., Hegland, P., Tysklind, M., 2007. Sources, fate, and toxic hazards of oxygenated polycyclic aromatic hydrocarbons (PAHs) at PAH-contaminated sites. AMBIO: J. Hum. Environ. 36, 475–485.

Maeda, A.H., Nishi, S., Ozeki, Y., Ohta, Y., Hatada, Y., Kanaly, R.A., 2013. Draft genome sequence of *Sphingobium* sp. strain KK22, a high-molecular-weight polycyclic aromatic hydrocarbon-degrading bacterium isolated from cattle pasture soil. Genome Announc 1.

Maeda, A.H., Kunihiro, M., Ozeki, Y., Nogi, Y., Kanaly, R.A., 2015. *Sphingobium barthaii* sp. nov., a high molecular weight polycyclic aromatic hydrocarbon-degrading bacterium isolated from cattle pasture soil. Int. J. Syst. Evol. Microbiol. 65, 2919–2924.

Maeda, A.H., Nishi, S., Hatada, Y., Ohta, Y., Misaka, K., Kunihiro, M., Mori, J.F., Kanaly, R.A., 2020. Chemical and genomic analyses of polycyclic aromatic hydrocarbon biodegradation in *Sphingobium barthaii* KK22 reveals divergent pathways in soil sphingomonads. Int. Biodeterior. Biodegradation 151, 104993.

Maeda, A.H., Nishi, S., Hatada, Y., Ozeki, Y., Kanaly, R.A., 2014. Biotransformation of the high-molecular weight polycyclic aromatic hydrocarbon (PAH) benzo[*k*]fluoranthene by *Sphingobium* sp. strain KK22 and identification of new products of non-alternant PAH biodegradation by liquid chromatography electrospray ionization tandem mass spectrometry. Microb. Biotechnol. 7, 114–129.

Mahbub, K.R., Krishnan, K., Megharaj, M., Naidu, R., 2016. Bioremediation potential of a highly mercury resistant bacterial strain *Sphingobium* SA2 isolated from contaminated soil. Chemosphere 144, 330–337.

Mallick, S., Chatterjee, S., Dutta, T.K., 2007. A novel degradation pathway in the assimilation of phenanthrene by *Staphylococcus* sp. strain PN/Y via meta-cleavage of 2-hydroxy-1-naphthoic acid: formation of trans-2,3-dioxo-5-(2′-hydroxyphenyl)-pent-4-enoic acid. Microbiology 153, 2104–2115.

Matsui, T., Yamada, N., Kuno, H., Kanaly, R.A., 2019. Formation of bulky DNA adducts by non-enzymatic production of 1,2-naphthoquinone-epoxide from 1,2-naphthoquinone under physiological conditions. Chem. Res. Toxicol. 32, 1760–1771.

Moody, J.D., Freeman, J.P., Fu, P.P., Cerniglia, C.E., 2004. Degradation of benzo[*a*]pyrene by *Mycobacterium vanbaalenii* PYR-1. Appl. Environ. Microbiol. 70, 340–345.

Mori, J.F., Kanaly, R.A., 2020. Multispecies diesel fuel biodegradation and niche formation are ignited by pioneer hydrocarbon-utilizing proteobacteria in a soil bacterial consortium. Appl. Environ. Microbiol. 87 (1).

Mori, J.F., Kanaly, R.A., 2021. Complete Genome Sequence of *Sphingobium barthaii* KK22, a high-molecular-weight polycyclic aromatic hydrocarbon-degrading soil bacterium. Microbiol. Resour. Announc. 10 (1).

M'rassi, A.G., Bensalah, F., Gury, J., Duran, R., 2015. Isolation and characterization of different bacterial strains for bioremediation of *n*-alkanes and polycyclic aromatic hydrocarbons. Environ. Sci. Pollut. Res. 22, 15332–15346.

Ní Chadhain, S.M., Moritz, E.M., Kim, E., Zylstra, G.J., 2007. Identification, cloning, and characterization of a multicomponent biphenyl dioxygenase from *Sphingobium yanoikuyae* B1. J. Ind. Microbiol. Biotechnol. 34, 605–613.

Nourse, B.D., Cox, K.A., Morand, K.L., Cooks, R.G., 1992. Collisional activation of pyrene and anthracene in an ion-trap mass spectrometer. J. Am. Chem. Soc. 114, 2010–2016.

Penning, T.M., 2014. Human aldo-keto reductases and the metabolic activation of polycyclic aromatic hydrocarbons. Chem. Res. Toxicol. 27, 1901–1917.

Pinyakong, O., Habe, H., Yoshida, T., Nojiri, H., Omori, T., 2003. Identification of three novel salicylate 1-hydroxylases involved in the phenanthrene degradation of *Sphingobium* sp. strain P2. Biochem. Biophys. Res. Commun. 301, 350–357.

Podgorski, D.C., Zito, P., Kellerman, A.M., Bekins, B.A., Cozzarelli, I.M., Smith, D.F., Cao, X., Schmidt-Rohr, K., Wagner, S., Stubbins, A., Spencer, R.G., 2021. Hydrocarbons to carboxyl-rich alicyclic molecules: a continuum model to describe biodegradation of petroleum-derived dissolved organic matter in contaminated groundwater plumes. J. Hazard. Mater. 402, 123998.

Rentz, J.A., Alvarez, P.J., Schnoor, J.L., 2008. Benzo[*a*]pyrene degradation by *Sphingomonas yanoikuyae* JAR02. Environ. Pollut. 151, 669–677.

Roy, M., Khara, P., Dutta, T.K., 2012. *meta*-cleavage of hydroxynaphthoic acids in the degradation of phenanthrene by *Sphingobium* sp. strain PNB. Microbiology 158, 685–695.

Schneider, J., Grosser, R., Jayasimhulu, K., Xue, W., Warshawsky, D., 1996. Degradation of pyrene, benz[*a*]anthracene, and benzo[*a*]pyrene by *Mycobacterium* sp. strain RJGII-135, isolated from a former coal gasification site. Appl. Environ. Microbiol. 62, 13–19.

Seo, J.-.S., Keum, Y.-.S., Hu, Y., Lee, S.-.E., Li, Q.X., 2006. Phenanthrene degradation in *Arthrobacter* sp. P1-1: initial 1,2-, 3,4- and 9,10-dioxygenation, and *meta*- and *ortho*-cleavages of naphthalene-1,2-diol after its formation from naphthalene-1,2-dicarboxylic acid and hydroxyl naphthoic acids. Chemosphere 65, 2388–2394.

Seo, J.S., Keum, Y.S., Hu, Y., Lee, S.E., Li, Q.X., 2007. Degradation of phenanthrene by *Burkholderia* sp. C3: initial 1,2-and 3,4-dioxygenation and *meta*-and *ortho*-cleavage of naphthalene-1,2-diol. Biodegradation 18, 123–131.

Song, M., Luo, C., Jiang, L., Zhang, D., Wang, Y., Zhang, G., 2015. Identification of benzo[*a*]pyrene-metabolizing bacteria in forest soils by using DNA-based stable-isotope probing. Appl. Environ. Microbiol. 81, 7368–7376.

Stolz, A., 2009. Molecular characteristics of xenobiotic-degrading sphingomonads. Appl. Microbiol. Biotechnol. 81, 793–811.
Stolz, A., 2014. Degradative plasmids from sphingomonads. FEMS Microbiol. Lett. 350, 9–19.
Sun, S.Y., Zhang, X., Zhou, Q., Chen, J.C., Chen, G.Q., 2008. Microbial production of *cis*-1,2-dihydroxy-cyclohexa-3,5-diene-1-carboxylate by genetically modified *Pseudomonas putida*. Appl. Microbiol. Biotechnol. 80, 977–984.
Takeshita, T., Kanaly, R.A., 2019. In vitro DNA/RNA adductomics to confirm DNA damage caused by benzo[*a*]pyrene in the Hep G2 cell line. Front Chem 7, 491.
Tian, Z., Vila, J., Yu, M., Bodnar, W., Aitken, M.D., 2018. Tracing the biotransformation of polycyclic aromatic hydrocarbons in contaminated soil using stable isotope-assisted metabolomics. Environ. Sci. Technol. Lett. 5, 103–109.
Tomiyama, Y., Takeshita, T., Mori, J.F., Kanaly, R.A., 2021. Functionalization of the model asphaltene 1-dodecylnaphthalene by *Pseudomonas aeruginosa* KK6 through subterminal metabolism. J. Petrol. Sci. Eng. 205, 108870.
Toyama, T., Furukawa, T., Maeda, N., Inoue, D., Sei, K., Mori, K., Kikuchi, S., Ike, M., 2011. Accelerated biodegradation of pyrene and benzo[*a*]pyrene in the *Phragmites australis* rhizosphere by bacteria-root exudate interactions. Water Res. 45, 1629–1638.
van Herwijnen, R., Wattiau, P., Bastiaens, L., Daal, L., Jonker, L., Springael, D., Govers, H.A.J., Parsons, J.R., 2003. Elucidation of the metabolic pathway of fluorene and cometabolic pathways of phenanthrene, fluoranthene, anthracene and dibenzothiophene by *Sphingomonas* sp. LB126. Res. Microbiol. 154, 199–206.
Verma, N., Pink, M., Rettenmeier, A.W., Schmitz-Spanke, S., 2012. Review on proteomic analyses of benzo[*a*]pyrene toxicity. Proteomics 12, 1731–1755.
Volpicella, M., Leoni, C., Manzari, C., Chiara, M., Picardi, E., Piancone, E., Italiano, F., D'Erchia, A., Trotta, M., Horner, D.S., Ceci, L.R, 2017. Transcriptomic analysis of nickel exposure in *Sphingobium* sp. ba1 cells using RNA-seq. Sci. Rep. 7, 1–10.
Xu, X., Zhang, J., Zhang, L., Liu, W., Weisel, C.P., 2004. Selective detection of monohydroxy metabolites of polycyclic aromatic hydrocarbons in urine using liquid chromatography/triple quadrupole tandem mass spectrometry. Rapid Commun. Mass Spectrom. 18, 2299–2308.
Yan, Z., He, Y., Cai, H., Van Nostrand, J.D., He, Z., Zhou, J., Krumholz, L.R., Jiang, H.L., 2017. Interconnection of key microbial functional genes for enhanced benzo[*a*]pyrene biodegradation in sediments by microbial electrochemistry. Environ. Sci. Technol. 51, 8519–8529.
Yu, C.L., Liu, W., Ferraro, D.J., Brown, E.N., Parales, J.V., Ramaswamy, S., Zylstra, G.J., Gibson, D.T., Parales, R.E., 2007. Purification, characterization, and crystallization of the components of a biphenyl dioxygenase system from *Sphingobium yanoikuyae* B1. J. Ind. Microbiol. Biotechnol. 34, 311–324.
Zeng, J., Zhu, Q., Li, Y., Dai, Y., Wu, Y., Sun, Y., Miu, L., Chen, H., Lin, X., 2019. Isolation of diverse pyrene-degrading bacteria via introducing readily utilized phenanthrene. Chemosphere 222, 534–540.
Zhao, Q., Yue, S., Bilal, M., Hu, H., Wang, W., Zhang, X., 2017. Comparative genomic analysis of 26 *Sphingomonas* and *Sphingobium* strains: dissemination of bioremediation capabilities, biodegradation potential and horizontal gene transfer. Sci. Total Environ. 609, 1238–1247.
Zhong, Y., Luan, T., Lin, L., Liu, H., Tam, N.F., 2011. Production of metabolites in the biodegradation of phenanthrene, fluoranthene and pyrene by the mixed culture of *Mycobacterium* sp. and *Sphingomonas* sp. Bioresour. Technol. 102, 2965–2972.
Zhong, Y., Luan, T., Wang, X., Lan, C., Tam, N.F., 2007. Influence of growth medium on cometabolic degradation of polycyclic aromatic hydrocarbons by *Sphingomonas* sp. strain PheB4. Appl. Microbiol. Biotechnol. 75, 175–186.
Zhu, F., Storey, S., Ashaari, M.M., Clipson, N., Doyle, E., 2017. Benzo[*a*]pyrene degradation and microbial community responses in composted soil. Environ. Sci. Pollut. Res. 24, 5404–5414.